DESIGN OF HIGH-PERFORMANCE REINFORCED CONCRETE SLENDER MEMBERS SUBJECTED TO UNIAXIAL LOADING AND BIAXIAL BENDING USING IS 456: 2000

Bajirao V. Mane[1*], Dr. Ajit N. Patil[2*]

Abstract:
The limit state design of reinforced concrete was introduced in India by IS 456 (1978). The fourth edition IS 456 (2000) incorporated important changes, such as durability considerations, revised formula for estimating modulus of elasticity, requirements for fire resistance, and regulations for deflections in flexural members. the Code recommends the use of the limit state design approach; However, it does not recommend the use of high-performance concrete for flexural members. The bending moment in the column may be caused by eccentric loading, lateral loads, or slenderness. This experimental study develops stress-block parameters for high-performance concrete based on tests on three series of specimens: Axially loaded columns, eccentrically loaded columns, and columns subjected to axial load with biaxially bending. The tests covered concrete strengths of 60 MPa to 80 MPa, with respect to cylinder and cube strengths. The experimental data of 81 columns (100mm x 150mm x 1300mm) is compared with the interaction curves developed using stress-block parameters of ACI 318 (2008), IS 456 (2000), and the present study. The new parameters are found to be more accurate. In simpler terms, the study developed new parameters for designing high-performance concrete flexural members, which are more accurate than the existing codes.

Keywords. Code; design; high performance concrete; stress-block parameters.

[1*,2*]Department of Civil Engineering, School of Engineering and Technology, DYPU, Ambi, Pune, 410506, India.
[1*]Department of Civil Engineering, Annasaheb Dange College of Engineering and Technology, Ashta, Sangli, 416301, India.

***Corresponding author:** Bajirao V. Mane, Ajit N. Patil
*Department of Civil Engineering, School of Engineering and Technology, DYPU, Ambi, Pune, 410506, India. [1]Email: bajimane9090@gmail.com, (https://orcid.org/0009-0004-0397-9784),
[2]Email: ajit.patil@dyptc.edu.in, ajitpatil2525@gmail.com
*Department of Civil Engineering, Annasaheb Dange College of Engineering and Technology, Ashta, Sangli, 416301, India.

DOI: 10.53555/ecb/2022.11.11.107

1. Introduction

The use of high-performance concrete (HPC) is increasing in recent years. Concrete strengths more than 80MPa are available. The use of HPC offers great advantage in the columns of high-rise structures and girders of large span bridges. In other countries there are many examples of use of this versatile material. In India, use of HPC is not common and there are very few examples such as use of 60MPa concrete in Kaiga nuclear power plant. HPC is not becoming popular in the absence of regulations in the form of code. The Indian standard code of practice for plain and reinforced concrete do mention use of high strength concrete in the new edition IS 456 (2000), without proper representation of it with design parameters such as flexural strength, modulus of elasticity and stress-block parameters. Literature indicates research on design parameters of high strength concrete were due to Ibrahim and MacGregor (1996, 1997), Bae and Bayrak (2003a, 2003b), Tan and Nguyon (2005), and Metrol et al. (2008). They have proved that ACI 318 is overestimating the moment capacities of the columns in flexure for high strength concrete. They tried to incorporate the conservativeness in the form of equivalent rectangular stress-block (ERSB) parameters α and β which reduces as strength of concrete increases (Nayak, C. B., Kharjule, K. ,2016).

If IS 456 (2000) is studied critically with respect to stress-block parameters the scenario is totally different. The stress-strain curve is lowered to $0.67f_{ck}$ and further lowered to $0.446f_{ck}$ as given in section 38.1 of IS 456 (2000). The reduction to 0.67 is due to size and shape effect and 0.446 is due to partial safety factor. The constant conversion factor of 0.8 for cylindrical to cube strength is questionable. Literature indicate no perfect relation between these two strengths, however, it was shown that the ratio increases with the increase in strength of concrete. The study of US Bureau reclamation factors (1992) and UNESCO (1971) conversion factor indicate this ratio as 0.85 and 0.80 respectively for specimen of 150 mm cube. Many others have suggested this value as 0.87, 0.77-0.96, and 0.85-0.88 by Cormack (1956), Evans (1944), and Gonnerman (1925) respectively for normal strength concrete (NSC) and high strength concrete indicating higher values for higher strength concrete (Nayak, C. B., Nerkar, S. ,2016). As far as partial safety factor is concerned, it is not essential at this stage. Due to sthese the ultimate load capacities cannot be compared by this code. However, the safety factors may be introduced at later stages of design as is found in ACI 318 (2008) as capacity reduction factor. The HPC is manufactured by exercising good quality control and there is no point in maintaining same factor of safety as that of normal strength concrete, otherwise it offsets the advantages of HPC.

In the present form of IS 456 (2000), the stress-block parameters are $k_1k_3 = 0.36$ and $k_2 = 0.42$, where the former is the area factor below the stress-strain curve and latter is the neutral axis factor. IS 456(2000) adopts the partly rectangular and partly parabolic variation of stress-strain curve along the neutral axis. This may be true for NSC but it does not represent the nature of HPC. The stress-strain relation becomes linear as strength of concrete increases. Adopting this kind of stress-block, leads to tedious calculations in the predictions of moment capacities especially in design of columns. Many codes such as ACI 318 (2008), AS 3600 (2001), NZS 3101 (2006) and Eurocode 02 (2004) adopted simpler stress-block which is called equivalent rectangular stress-block (ERSB). All the codes and researchers adopt conservative values of k_1k_3 but not to this extent of IS 456 (2000). The constant value of k_2 is also objectionable as far as higher strength concrete is concerned. In fact this value should decrease as strength of concrete increases. Therefore, constant value of $k_2 = 0.42$ creates lower lever arm and adds to the conservativeness of predictions.

IS code specifying the ultimate strain as 0.0035 in pure flexure. The clause 38.1e, the maximum compressive strain is 0.002 and it is 0.0035 minus 0.75 times the strain at the least compressed fiber when the member is subjected to axial compression and bending. Even though we find ultimate strain of the order of 0.0042 for higher strength concrete, many codes restrict it to 0.003. The Indian code does not specify the ultimate strain for the columns failing in tension.

The other design parameters such as flexural strength and modulus of elasticity were based on the tests on NSC. These parameters should also be modified for HPC. Therefore, the IS 456 (2000) in the present form does not represent the HPC and hence may need necessary modifications.

2. Research Significance

After 22 years, IS 456 (1978) was revised with main emphasis on durability and some other significant changes regarding estimation of modulus of elasticity, deflections of flexural members, fire resistance etc. During this period and next decade there was vast improvement in the state-of-art of high-performance concrete, but still left un-represented in the code. At the same

time many other codes such as ACI 318 (2008), AS 3600 (2001), NZS 3101 (2006) and Eurocode 02 (2004) etc., have incorporated changes in their code for HPC. Use of HPC can lead to smaller sections in high rise buildings, leading to saving of material, especially cementitious material conserving it for future generations. The HPC is also consuming waste materials such as fly ash, silica fume, GGBS, rice husk ash. Hence, use of this is not only economical but also environment friendly. Lack of representation of HPC in the code may deprive the designers to use it in the structures. This paper, gives analytical equations for estimating modulus of elasticity, flexural strength and stress-block parameters based on an extensive experimental set up. This research may become the base for future revision of IS 456 (2000).

3. Experimental Program

3.1 *Materials and Mix proportioning*

The precise combination of constituent materials required to produce a concrete mixture with the desired characteristics at the most economical cost is determined through a process known as mix proportioning. High-performance concrete (HPC) is created through a meticulous selection of its components. Throughout the investigation, commercially available ordinary Portland cement of 53 grade (Ultratech cement) that complies with the relevant Indian standard code IS 12269 (1987) was employed. Crushed basalt stone aggregates were utilized for the current study. To produce 60 MPa and 12.5 MPa concrete, respectively, the maximum aggregate size was 20 mm and 12.5 mm. Locally available sand extracted from the Krishna River was used. The sand employed complies with grading zone II of IS 383 (1970). To achieve the required strength, fly ash, silica fume (Elkem), and high-range water-reducing admixtures (Glenium B233) were employed. In accordance with the technique suggested by Aitcin (1998), concrete mix designs for five target strengths were created, as shown in Table 1.

Table 1. Mix proportioning for five target compressive strengths

Materials	Compressive Strength in MPa		
	60	**70**	**80**
W/C	0.44	0.39	0.36
Cement, kg/m^3	366	405.11	441
Fine Aggregate, kg/m^3	693.24	654.90	615.78
Coarse Aggregate, kg/m^3	1087.79	1087.79	1087.79
Water, kg/m^3	162.63	158.23	157.24
Metakaolin, kg/m^3	---	----	----
Fly ash or silica fume kg/m^3	91.42	101.29	110
HRWR (Master Glenium Sky 8654) in %	0.4	0.42	0.45

3.2 *Casting of specimens*

For the present experimental work, a 250 kg capacity ribbon concrete mixer was employed to mix the concrete. To mimic real-world construction practices, all specimens were cast vertically. The observed slump values ranged from 100 mm to 150 mm. An internal electric needle vibrator was utilized to consolidate the concrete in three layers. Each layer of concrete was thoroughly compacted to eliminate entrapped air. Three cubes (150 mm × 150 mm × 150 mm) and three cylinders (150 mm × 300 mm) were cast with each specimen to evaluate the concrete's strength in the columns and for testing alongside the column. For 120 MPa concrete, the companion cubes and cylinders were sized at 100 mm × 100 mm × 100 mm and 100 mm × 200 mm, respectively. The concrete specimens and their corresponding cubes and cylinders were cured by covering them in wet gunny bags and continuously watering for 28 days. Before testing, the ends of each specimen were carefully ground to ensure their verticality in the testing machine. To assure that the ends were perpendicular to the sides, the ends of all cylinders were also ground.

3.3 *Instrumentation*

The primary object of instrumentation in these types of specimens was to measure and record the strain on tension, compression faces and to plot the strain distribution profile across the section. Three types of displacement measuring devices were employed, namely, LVDT's (displacement-based transducers), pi-gauges (strain based transducers) and dial gauges. Dial gauges were used where displacement was expected more than 10mm such as for central displacement in columns and beams. Due care was taken for rigid application of these devices and also the gauge lengths were so selected (200mm or 250mm) to minimize the effect of localized strain near the cracks. Typical test set up is as shown in Figs.1-3.

In fixed neutral axis specimens, strain measurements were obtained using one linear variable displacement transducer (LVDT) on the tension face, two LVDTs on the compression face, and two pi-gauges on the front face. For eccentrically loaded columns, strain measurements were obtained using one pi-gage and one LVDT on each compression and tension face, along with an additional LVDT at the center of the front face. The average readings of two transducers were used when two displacements were measured on the compression and tension faces. Strain profiles for beams were determined using three pi-gauges and two LVDTs across the cross-section. Deflections under the loads and at the center of the beams were measured using two LVDTs and one dial gauge, respectively.

3.4 *Test Specimens and set up*

The experimental program consists of testing of HPC members in flexure. Three series of test specimen were used to determine the compressive stress- block such as un-reinforced columns (fixed neutral axis specimen) and eccentrically loaded columns and beams in flexure.

3.4.a. *Fixed neutral axis specimens*

Eighteen unreinforced concrete columns measuring 100mm × 150mm × 1300mm were cast. Both ends of the specimens were reinforced with four 8mm, four 10mm, and four 12mm diameter longitudinal bars bent into a U-shape with well-distributed transverse reinforcement. Additionally, both ends were heavily confined with 12mm thick steel tubes to prevent premature failure. Primary load P1 and secondary load P2 were applied monotonically in a manner that maintained zero strain on the exterior tension face. Two fabricated horizontal steel arms were used to apply the secondary load. Both steel arms were adjusted to a height approximately equal to the height of the column and held together by a 25mm threaded rod passing through them. A load cell and hydraulic jack were placed above the top arm, passing through the rod. The specimen was then positioned in the compression testing machine, aligned, and leveled on the roller connection. Another roller connection was placed at the top of the specimen with an external 2000kN load cell above it. Two Teflon sheets were used over the top and bottom of the specimen (Nayak, C. B., Wadgave, P. ,2016). Both arms were connected to the specimen through bolts and nuts under an initial load on the specimen. Subsequently, the load was released, and the machine was restarted with the initial readings set to zero. Rigidity of the assembly was carefully ensured. Then, the secondary load was applied to maintain the neutral axis on the exterior tension face of the specimen. The primary load was applied at a rate of 0.005mm/sec through a servo-controlled compression testing machine of 3000kN capacity. The data was captured in a 12-channel data logging system with an interface to the computer. Fig. 1 illustrates the test setup.

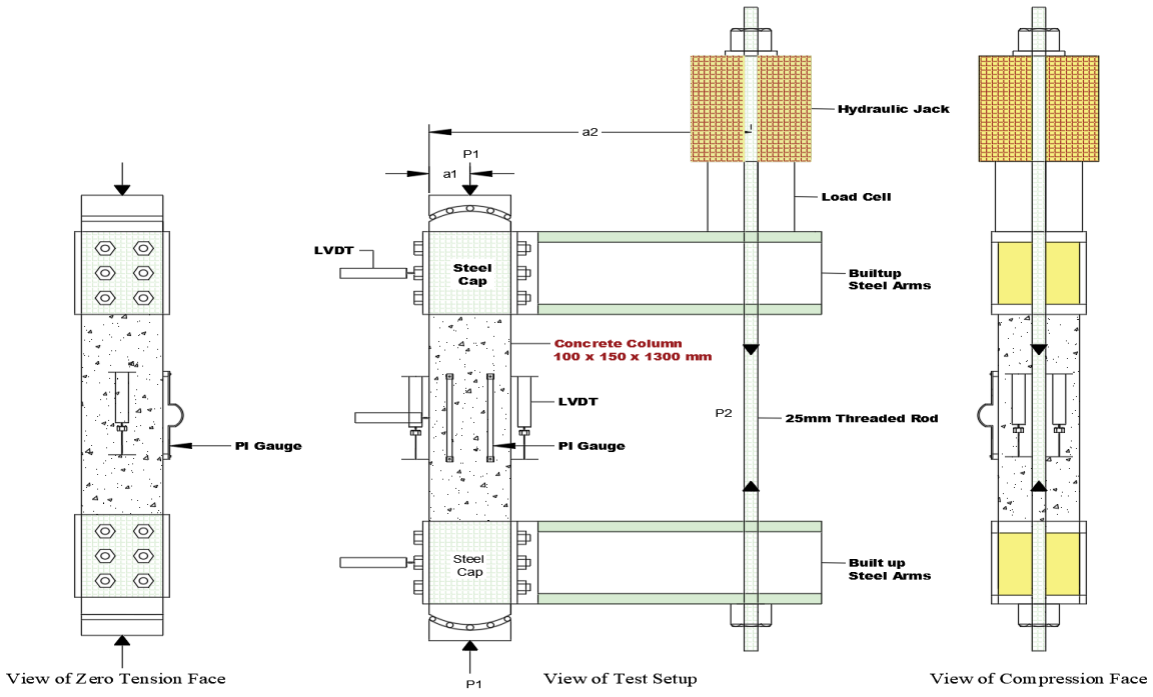

Fig.1 Test set up of fixed neutral axis specimens

3.4.b. *Eccentrically loaded columns*

Fourteen reinforced concrete columns, ranging in strength from 60MPa to 120MPa, measuring 100mm × 150mm × 1300mm, were cast. The specimens had 2.01%, 3.14%, and 4.52% longitudinal steel (four bars of 8mm, 10mm, and 12mm diameter) and lateral ties of 8mm diameter at 100mm center-to-center spacing. The columns were tested at eccentricities of 20% of the least lateral dimension, where h = 150mm. A specially designed plate and load knife edges were employed to apply the load at specific eccentricities for eccentrically loaded columns. The two ends of the columns were securely confined by angle capping to prevent the slippage of the plates used to apply the eccentricities. Figure 3 illustrates a typical test setup for eccentrically loaded columns.

Table 4 Details of Column Specimens

Sr. No.	Concrete Grade	Longitudinal Reinforcement	% of Reinforcement	Loading Conditions and [Column Designation (No.'s)]		
				Axial	Uni-Axial	Bi-Axial
01	**M60**	4# 8mm	2.01	R60IA (3)	R60IU (3)	R60IB (3)
		4# 10mm	3.14	R60IIA (3)	R60IIU (3)	R60IIB (3)
		4# 12mm	4.52	R60IIIA (3)	R60IIIU (3)	R60IIIB (3)
02	**M70**	4# 8mm	2.01	R70IA (3)	R70IU (3)	R70IB (3)
		4# 10mm	3.14	R70IIA (3)	R70IIU (3)	R70IIB (3)
		4# 12mm	4.52	R70IIIA (3)	R70IIIU (3)	R70IIIB (3)
03	**M80**	4# 8mm	2.01	R80IA (3)	R80IU (3)	R80IB (3)
		4# 10mm	3.14	R80IIA (3)	R80IIU (3)	R80IIB (3)
		4# 12mm	4.52	R80IIIA (3)	R80IIIU (3)	R80IIIB (3)
Total No. of Columns = 81 no.'s						

Designations:	
R: Rectangular Column of size 100m x 100mm x1300mm	A: Axially Loaded Column
I: Longitudinal Reinforcement 2.01%	U: Uniaxially Loaded column
II: Longitudinal Reinforcement 3.14%	B: Biaxially Loaded Column
III: Longitudinal Reinforcement 4.52%	60, 70 and 80: Strength of HPC.

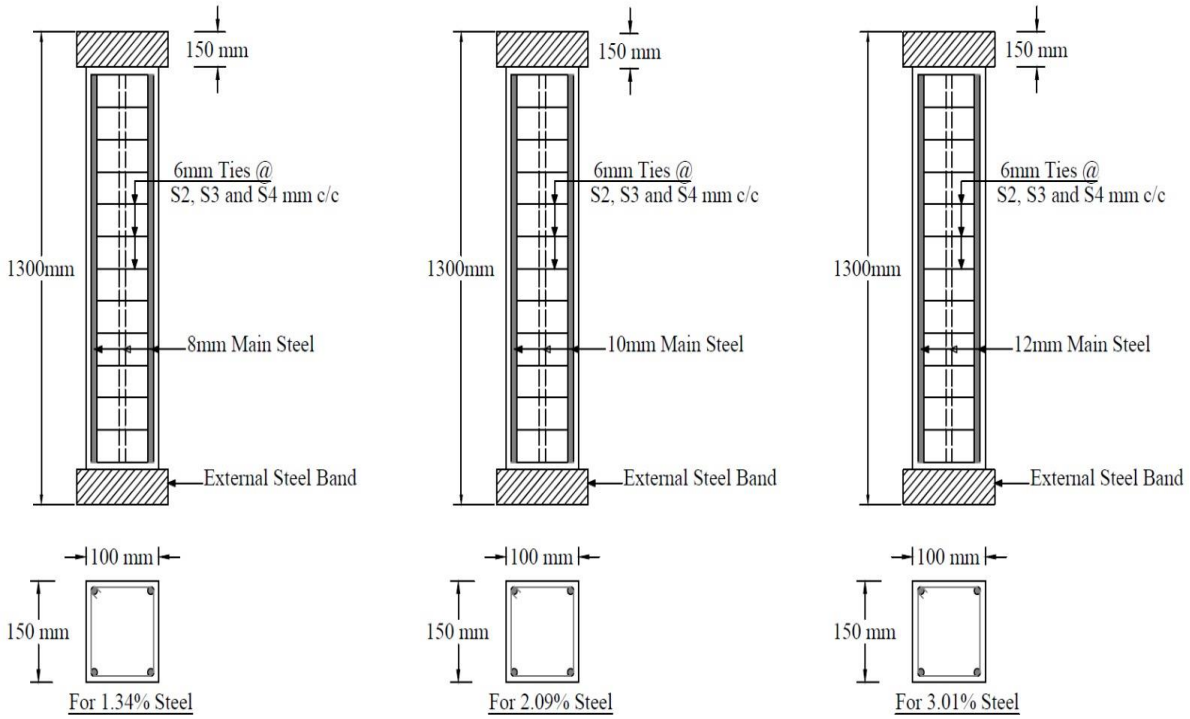

Fig. 3 Reinforcement details and test set up of eccentrically loaded column

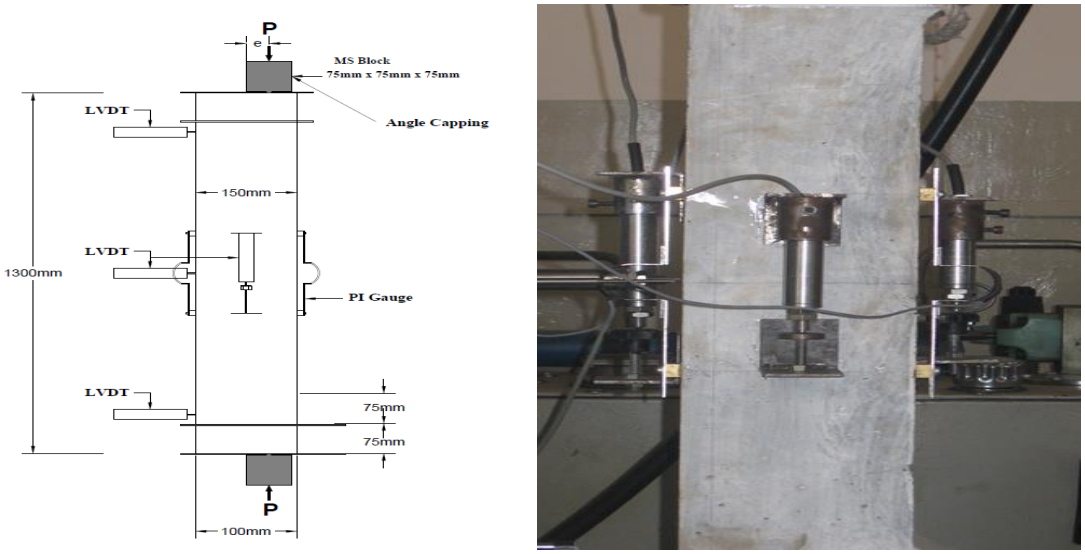

Fig. 4 Schematic diagrams for LVDT arrangement

4. Test results and Discussions

4.1 *Some mechanical properties of HPC*

4.1a *Ratio of cylindrical to cube compressive strength*

Concrete compression testing standards vary across countries, primarily in the type of specimen used. Cylindrical specimens (150mm×300mm) are employed in Australia, Canada, France, New Zealand, and the United States, while cube specimens (150mm or 100mm) are utilized in much of Europe, including Great Britain and Germany, and in India. Due to their differing shapes, sizes, and testing conditions, establishing an exact analytical equation relating their strengths is challenging. Researchers like Neville (1981), Cormack (1956), Evans (1944), and Gonnerman (1925) have attempted to link them analytically and experimentally, with Neville (1981) and L'Hermite (1955) providing analytical representations. Despite ongoing debates, the cylinder-cube strength ratio typically falls between 0.8 and 0.90, with a higher ratio observed for higher strength concrete. Figure 4 illustrates the conversion factor for high-strength concrete derived from the present study, which is analytically represented by Eq.1. Considering the overall trend, it is recommended to adopt a conversion factor of 0.8 for normal strength concrete (NSC) up to 40MPa and 0.85 for higher strength concrete.

$$f_c' = 0.88\, f_{cu} \qquad (1)$$

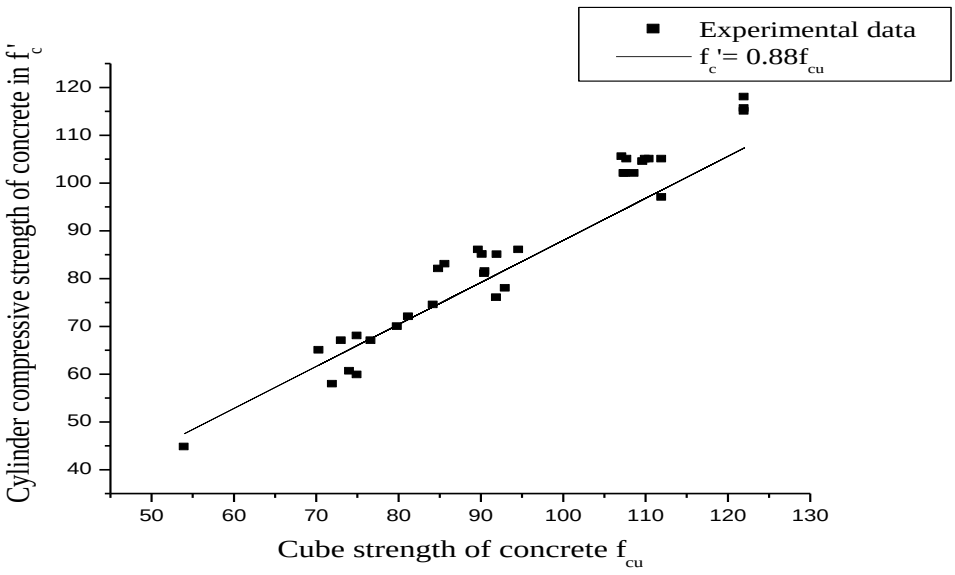

Fig. 5 Relation between cylinder strength and cube compressive strength of HPC

4.1b *Modulus of rupture*

For symmetrical two-point loading, the critical crack can arise at any section that is not strong enough to withstand the stress within the middle third, where the bending moment is at its maximum. It is anticipated that two-point loading will produce a lower modulus of rupture value than center-point loading. IS 516 (1959) mandates two-point loading for flexural testing. Based on the experimental findings presented in Table 2 of this study, the modulus of rupture can be expressed analytically in terms of the concrete's cylinder and cube compressive strengths as follows:

$$f_{r1} = 0.946\sqrt{f_c'} \quad in MPa \qquad (2)$$

$$f_{r2} = 0.90\sqrt{f_{cu}} \quad in MPa \qquad (3)$$

The expression for modulus rupture as per IS 456 (2000), in section 6.2.2 is as given below, where f_{ck} is characteristic strength of concrete.

$$f_r = 0.70\sqrt{f_{ck}} \quad in MPa \qquad (4)$$

The values of modulus of rupture determined as per Eq. 4, yields lower values of f_r for HPC as compared to Eq. 3.

4.1c *Modulus of elasticity of concrete*

An analysis of the stress-strain curves generated in this study revealed the elastic modulus at 40% stress level for various concrete grades, as presented in Table 2. The elastic modulus, Ec, for each specimen was plotted against the corresponding concrete strength, fcu, as shown in Figure 5.

Given the strong correlation between concrete strength and the modulus of elasticity, numerous attempts have been made to formulate their relationship. Figure 6 compares the predictions of some existing experimental data with the present test data. The relationships for Ec were obtained with respect to cylinder and cube strength of concrete, as shown below:

$$E_{C1} = 5050\sqrt{f_c'} \quad in MPa \qquad (5)$$

$$E_{C2} = 4800\sqrt{f_{cu}} \quad in MPa \qquad (6)$$

The expression for modulus rupture as per IS 456 (2000), in section 6.2.3.1 is as given below, where f_{ck} is characteristic strength of concrete.

$$E_c = 5000\sqrt{f_{ck}} \quad in MPa \qquad (7)$$

The modulus of elasticity values determined in this study fall within the range of 40 to 57 GPa for concrete strengths ranging from 60 to 80 MPa. In contrast, the values obtained using reference Eq. 7 are higher than those obtained using Eq. 6. This suggests that IS 456 (2000) overestimates Ec for HPC.

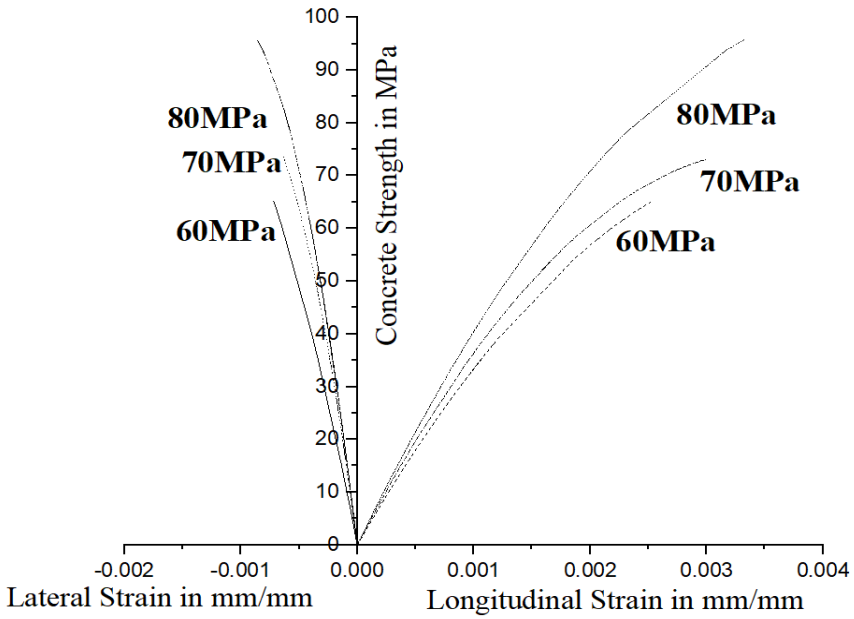

Fig. 5 Typical stress-strain relationships of concrete of strength 60MPa-80MPa

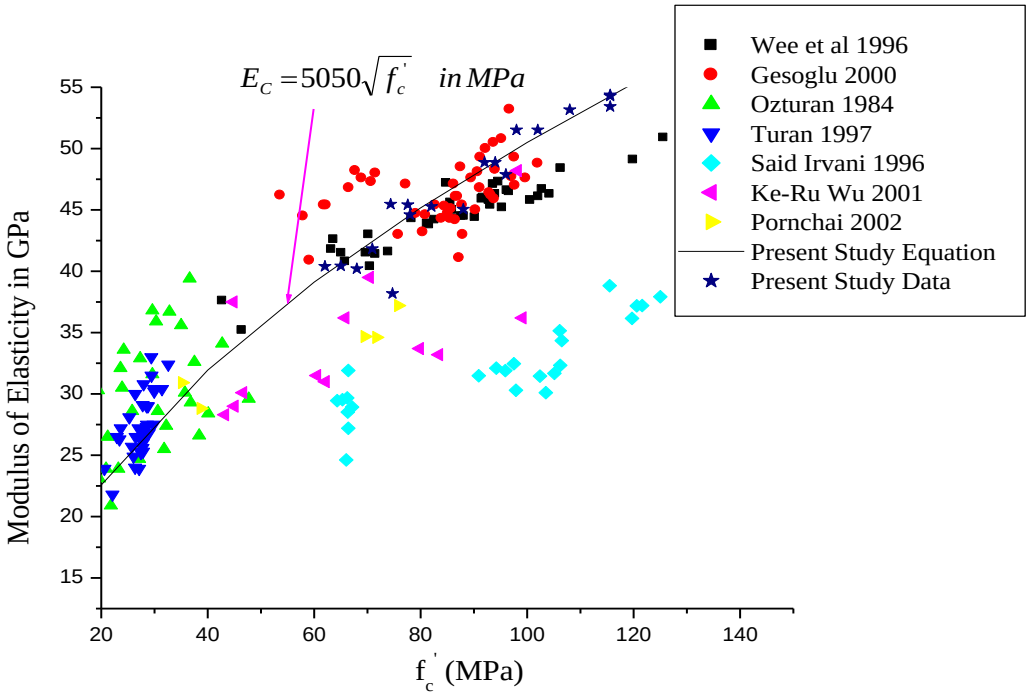

Fig. 6. Values of elastic modulus of present research and others in the literature

Table 2. Experimental values of Split and flexural tensile strengths

Strength of Concrete in MPa	Cube Strength f_{cu} in N/mm^2	Cylindrical Strength f_c' in N/mm^2	Flexural Strength f_r in N/mm^2	Ultimate Strain in mm/mm	Elastic Modulus $E_c$in GPa
60	75.55	62.00	7.20	0.0023	40.40
60	74.66	64.00	7.48	0.0028	41.84
60	75.11	67.71	7.28	0.0027	40.20
60	74.66	68.00	7.28	0.0026	40.43
60	77.33	65.00	7.46	0.0024	38.18
70	78.83	67.00	42.40	70	78.83
70	80.86	70.90	44.84	70	80.86
70	79.51	68.00	42.20	70	79.51
70	80.10	67.00	44.43	70	80.10
70	78.63	70.71	43.18	70	78.63
80	83.50	76.00	8.44	0.0030	45.42
80	84.00	78.00	8.52	0.0026	45.05
80	92.22	85.00	8.60	0.0027	45.47
80	89.33	75.00	8.53	0.0030	44.61
80	87.77	74.00	8.60	0.0029	45.27

4.2 *Stress-block parameters*

The stress-block parameters k1, k2, and k3 are determined based on the ultimate strain in concrete. The maximum stress factor k3 is obtained by dividing the maximum stress developed in the specimen by the cylindrical strength of concrete, and the area shape factor k1 is obtained by dividing k1k3 by k3. For reinforced columns under eccentric loading, the loads and moments carried by the longitudinal reinforcement are subtracted out based on the strain profile when calculating the stress-strain distribution and stress-block parameters. The equivalent rectangular stress-block parameters are derived from the generalized stress-block parameters using the equations given below:

$$\alpha = \frac{k_1 k_3}{2k_2} \quad (8)$$

$$\beta = 2k_2 \quad (9)$$

4.2a *Stress-block parameters with respect to cylinder strength of concrete*

The values of k1k3 and k2 obtained in this study, along with data collected from other researchers, are plotted against fc' in Figures 7 and 8. The

results demonstrate that k1k3 and k2 are functions of concrete strength, fc'. This is evident due to the fact that the area below the stress-strain diagram decreases as it becomes more linear for higher strength concrete. The stress-block parameters proposed with respect to cylindrical strength are:

k1k3 = 0.925 - 0.0047 fc'

k2 = 0.45 - 0.0115 fc'

These equations provide a method for calculating the stress-block parameters for concrete of varying strengths.

$$\alpha = 0.85 - \frac{1}{1000}\left(f_c' - 20\right) \quad 0.85 \geq \alpha \geq 0.75 \qquad (10)$$

$$\beta = 0.85 - \frac{1}{500}\left(f_c' - 20\right) \quad 0.85 \geq \beta \geq 0.67 \qquad (11)$$

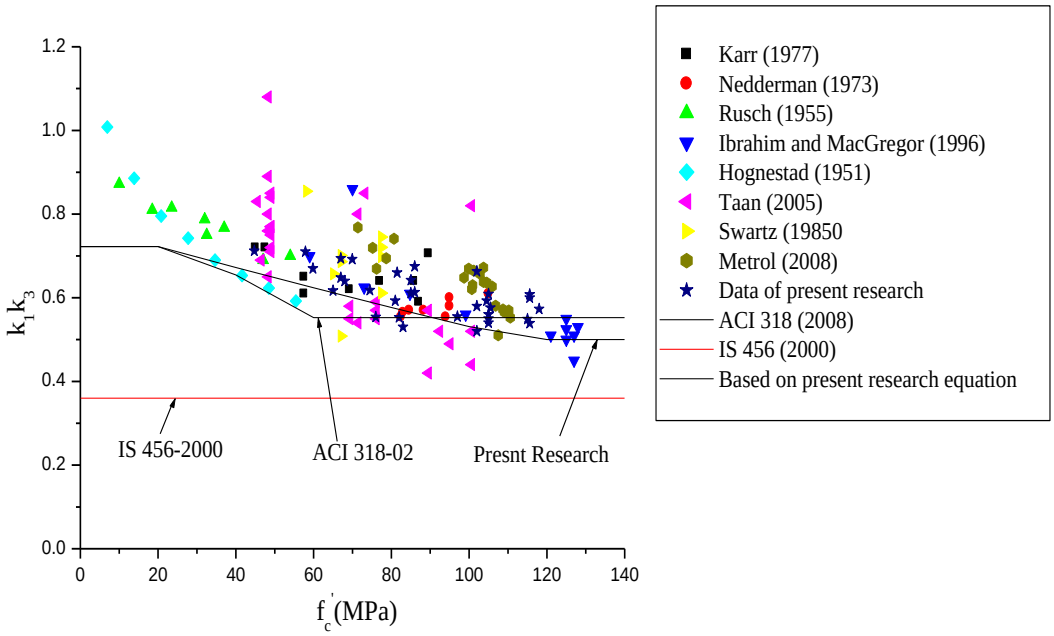

Fig.7. Proposed relationship with past and present data of k_1k_3

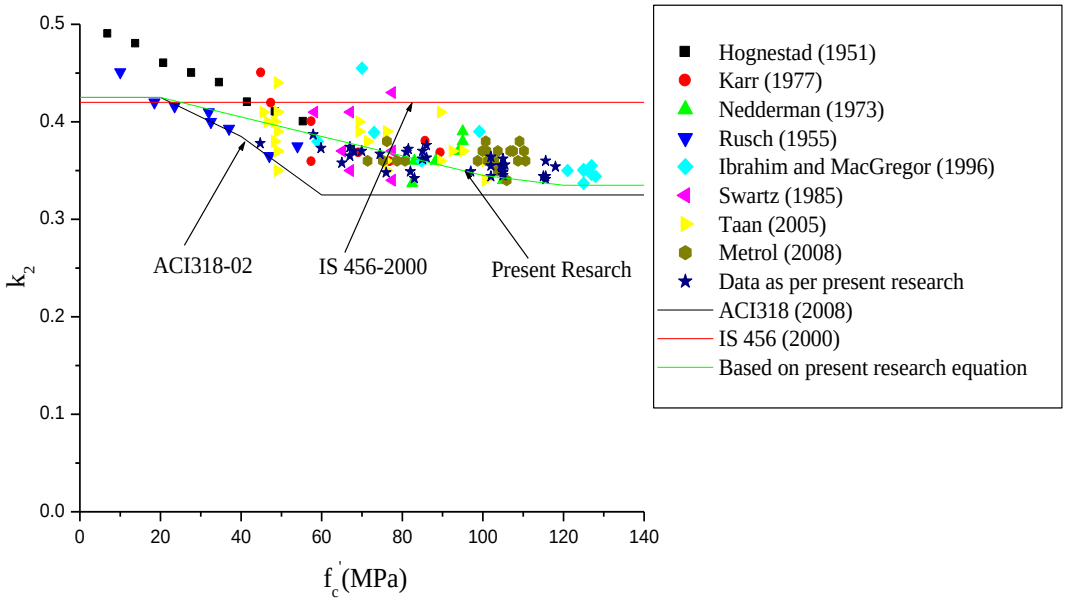

Fig.8 Proposed relationship with past and present data of k_2

4.2.b. ***Stress-block parameters with respect to cube strength of concrete***

IS 456 (2000) proposes a partly rectangular and partly parabolic variation for stress-block across the neutral axis, as illustrated in Figure 9. The code reduces ultimate stress to 0.67fck. This reduction factor is determined using a size effect factor of 0.85 and a relationship between cylinder and cube strength of 0.8. Applying a conversion factor of 0.8 for normal strength concrete (NSC) without strength reduction or a partial safety factor, the area below the stress-strain diagram is 0.645 (Figure 9a). For medium strength concrete (60 MPa - 80 MPa), the stress-block proposed by IS 456 is not applicable, as the stress-strain behavior becomes parabolic without a straight, flattened part after the peak stress. For this strength range, using a conversion factor of 0.85, the area below the curve becomes 0.566 (Figure 9b). For higher strength concrete, the stress-strain diagram becomes linear, and with a conversion factor of 0.85, the area below the curve becomes 0.425 (Figure 9c). These results demonstrate that the area below the stress-strain diagram for the corresponding stress-block varies from 0.645 to 0.425 when cube strength of concrete is considered.

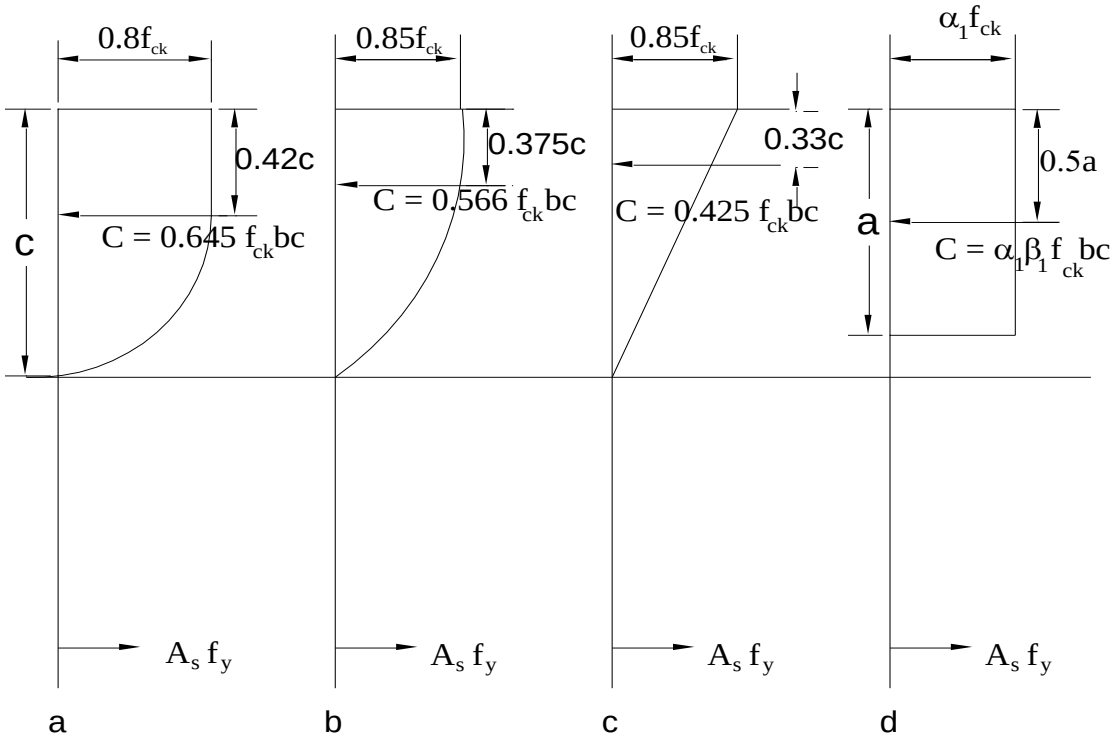

Fig. 9. Different types of stress-blocks

Maintaining the same neutral axis factor as derived with respect to cylinder strength results in a lower value of k2, leading to a larger lever arm. Consequently, it should be modified with respect to cube strength of concrete. The stress-block parameters k1k3 and k2 obtained in the present study are presented in Figures 10 and 11, respectively, with respect to cube compressive strength of concrete. he neutral axis factor in terms of β1 can be varied from 0.85 to 0.67. Using these values of β1, the value of α1 is calculated and fixed within the range of 0.75 to 0.69. The equations for these parameters with respect to cube strength are given below:

k1k3 = 0.825 - 0.0035 fc'
k2 = 0.24 - 0.0035 fc'
α1 = 0.2625 - 0.0065 fc'

These equations provide a method for calculating the stress-block parameters for concrete of varying strengths based on cube strength.

$$\alpha_1 = 0.75 - \frac{1}{1000}(f_{cu} - 20) \quad 0.75 \geq \alpha \geq 0.69 \qquad (12)$$

$$\beta_1 = 0.85 - \frac{1}{600}(f_{cu} - 20) \quad 0.85 \geq \beta \geq 0.67 \qquad (13)$$

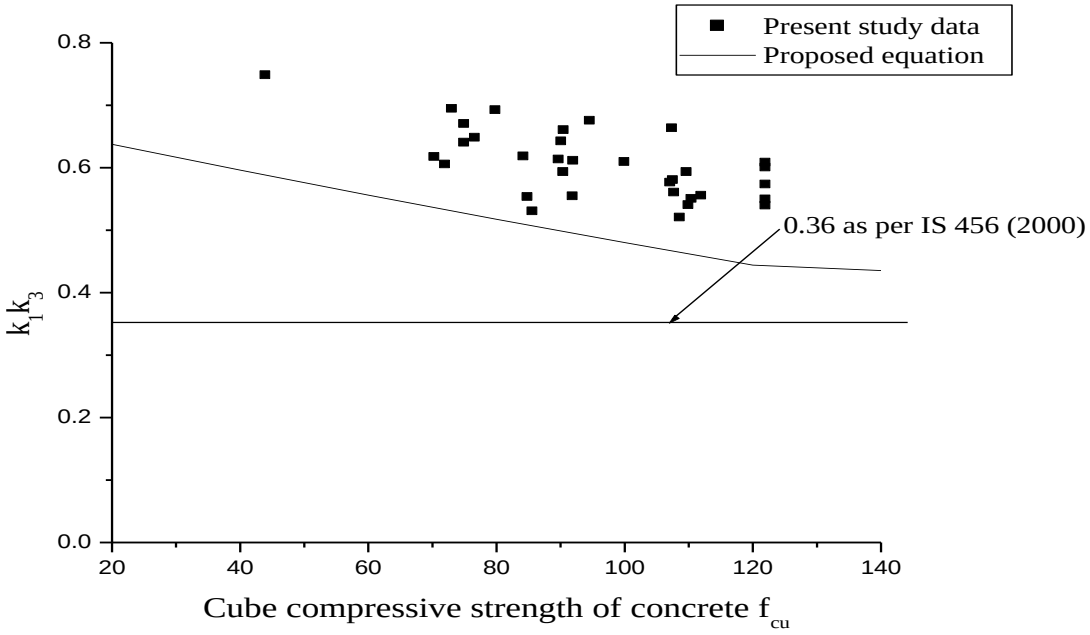

Fig 10. Proposed relation for k_1k_3 with present experimental data

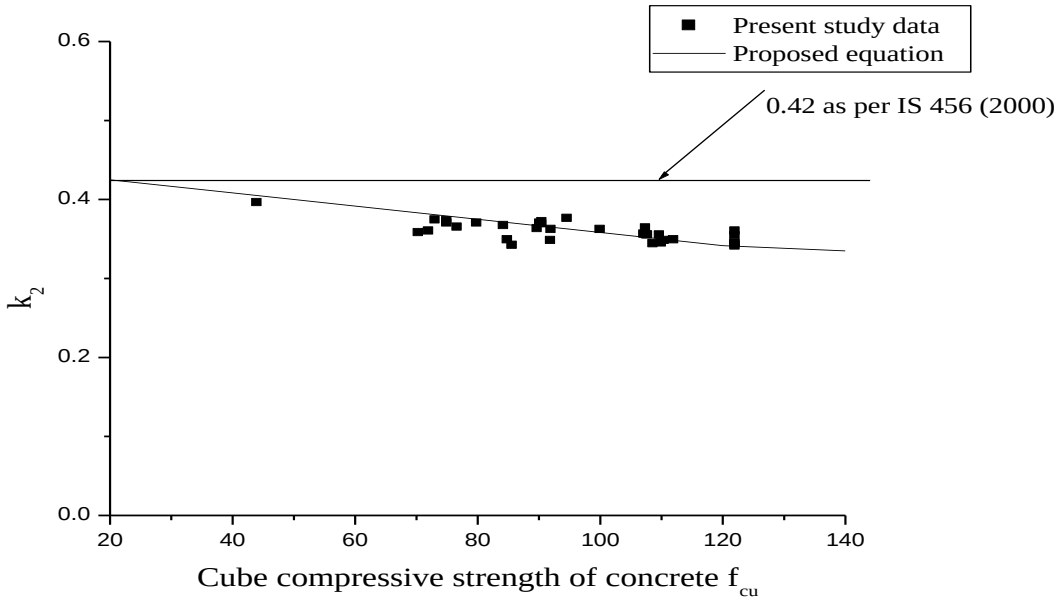

Fig 11. Proposed relation for k_2 with present experimental data

The equation for k1k3 produces reasonably conservative values for a given concrete strength, as shown in Figure 10. The other parameter, β1, aligns with the experimental results, as depicted in Figure 11. This alignment is unsurprising, given that the neutral axis factor remains constant at all stress levels. It should not be reduced solely because the k1k3 values are conservative.

5. Comparison of proposed stress-block parameters with interaction curves

Moment interaction curves were constructed using the stress-block parameters of ACI 318 (2008), IS 456 (2000), and the parameters proposed in the present study. The test data were compared, as shown in Figures 12-15. Over 50% of the predictions of column capacity using ACI 318 (2008) were non-conservative. IS 456 (2000) is overly conservative, indicating that the code does not adequately represent higher strength concrete. The parameters proposed by the authors based on cylindrical strength only predict one data point for 80 MPa concrete below the interaction curve. The new parameters based on cube strength align closely with the curve proposed by the authors based on cylindrical strength up to 80 MPa, but

become conservative for strengths above 70 MPa. This could be due to the assumed conversion factor of 0.85 from cylindrical to cube strength.
The proposed equations with respect both cylinder and cube strength for stress-blocks parameters show good agreement with the tested data acquisition various modes of failures except little more conservativeness for the latter beyond 80MPa.

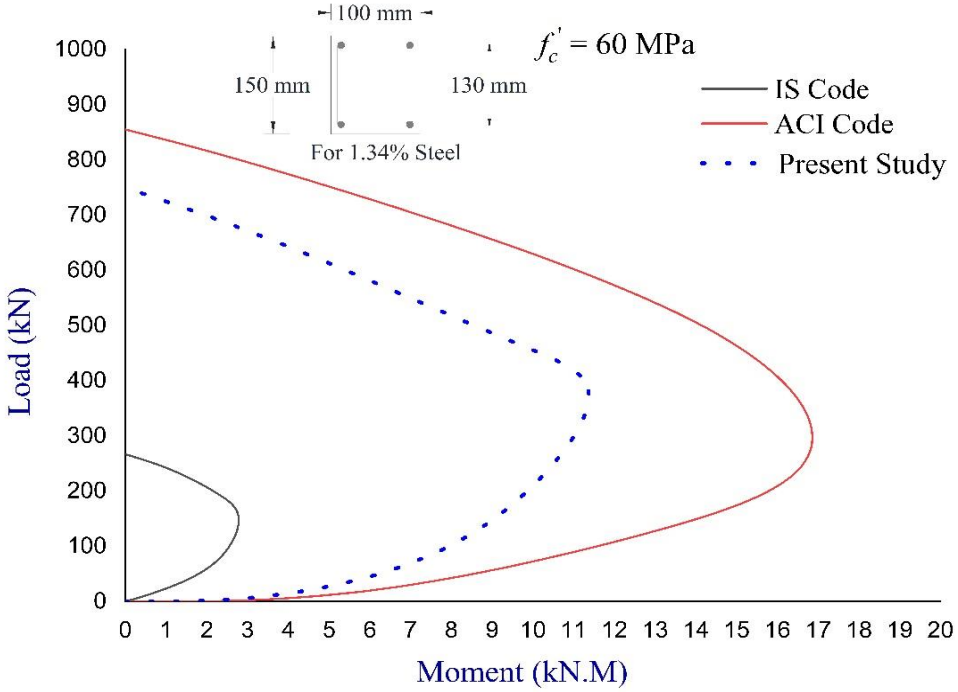

Fig. 12. Moment Interaction curve for 60MPa concrete (1.34%) Uniaxial Loading

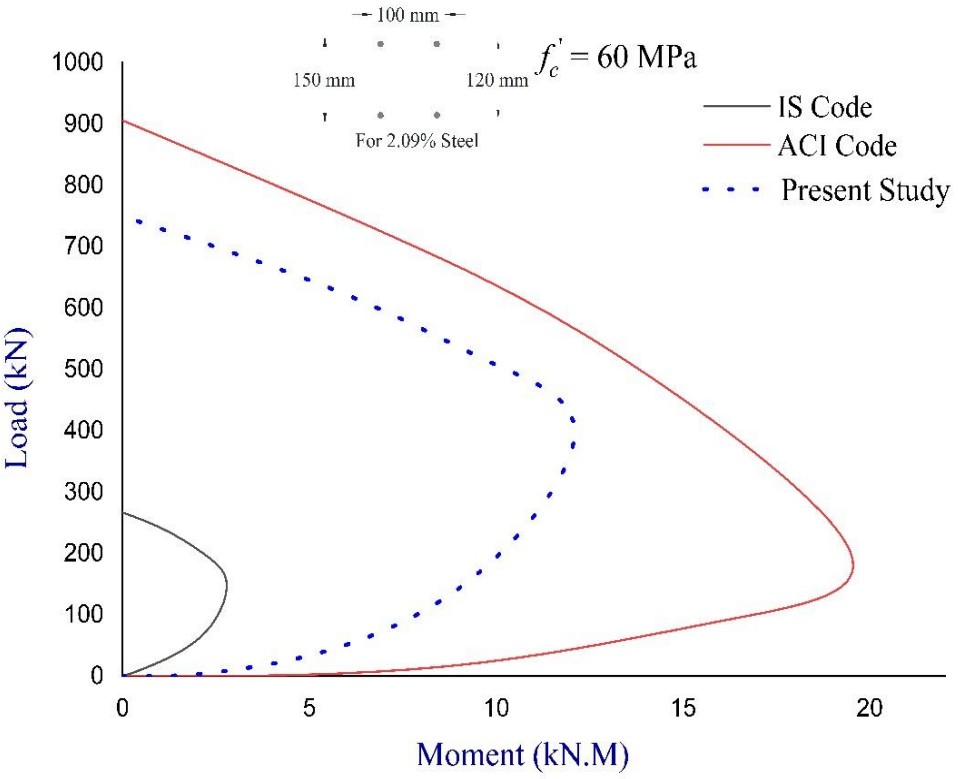

Fig. 13. Moment Interaction curve for 60MPa concrete (2.09%) Uniaxial Loading

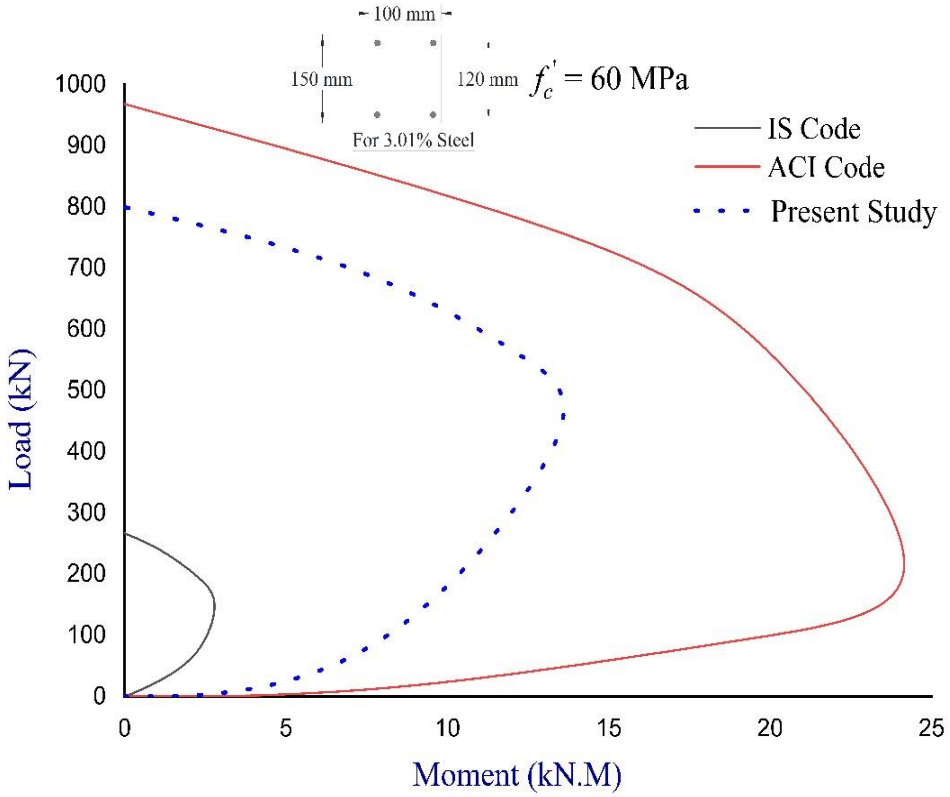

Fig. 14. Moment Interaction curve for 60MPa concrete (3.01%) Uniaxial Loading

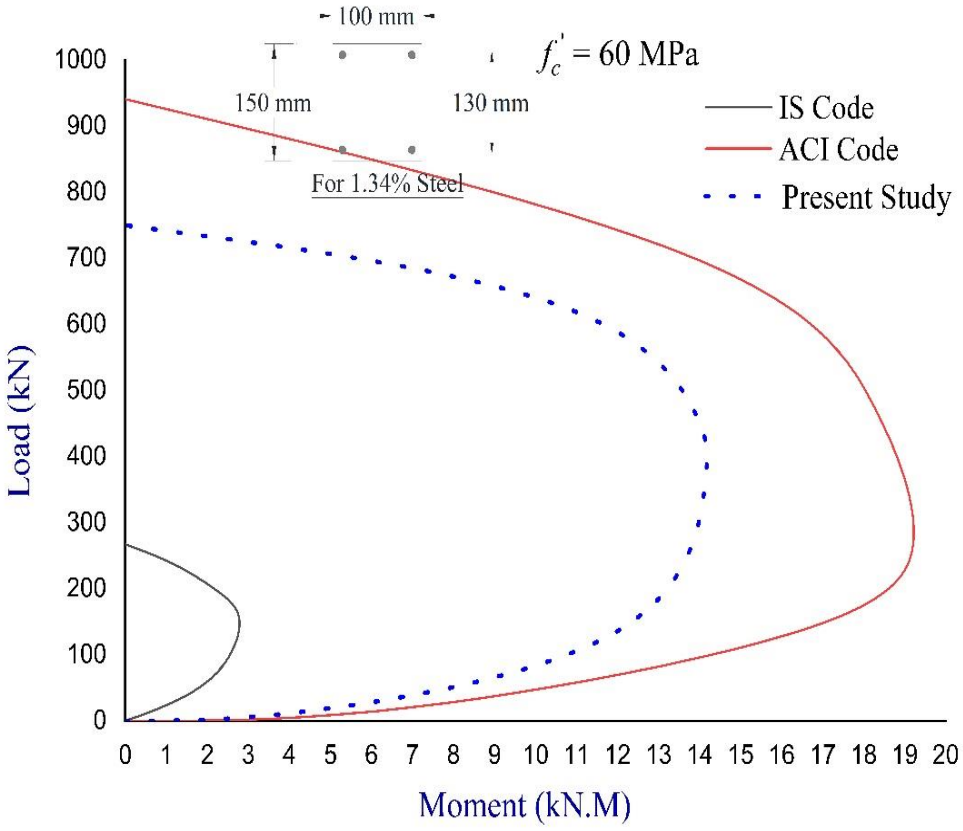

Fig. 15. Moment Interaction curve for 60MPa concrete (1.34%) Biaxial Loading

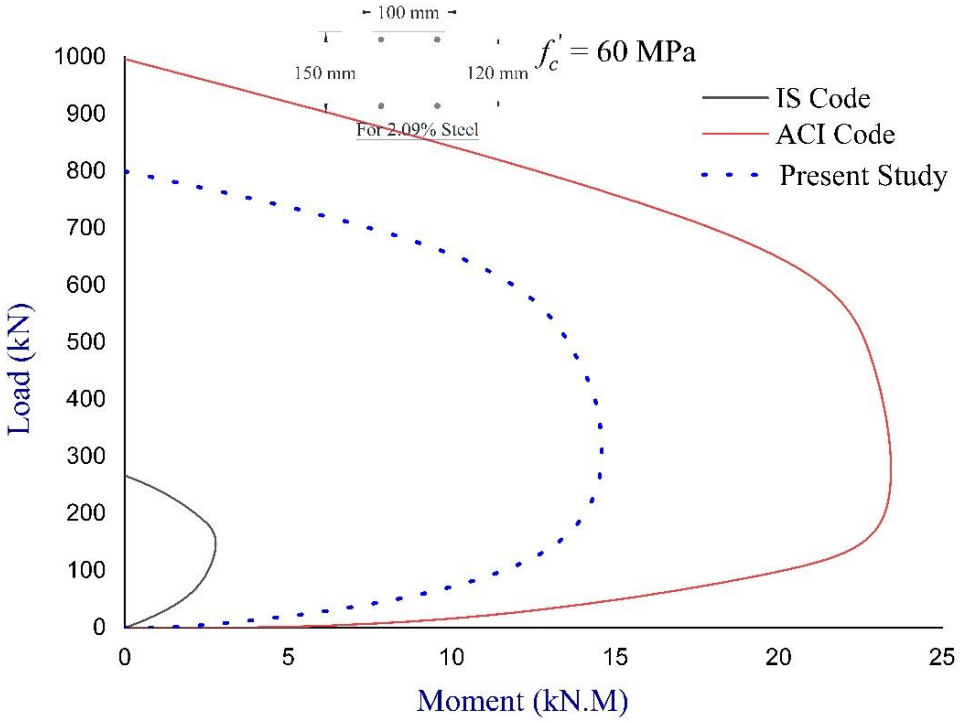

Fig. 16. Moment Interaction curve for 60MPa concrete (2.09%) Biaxial Loading

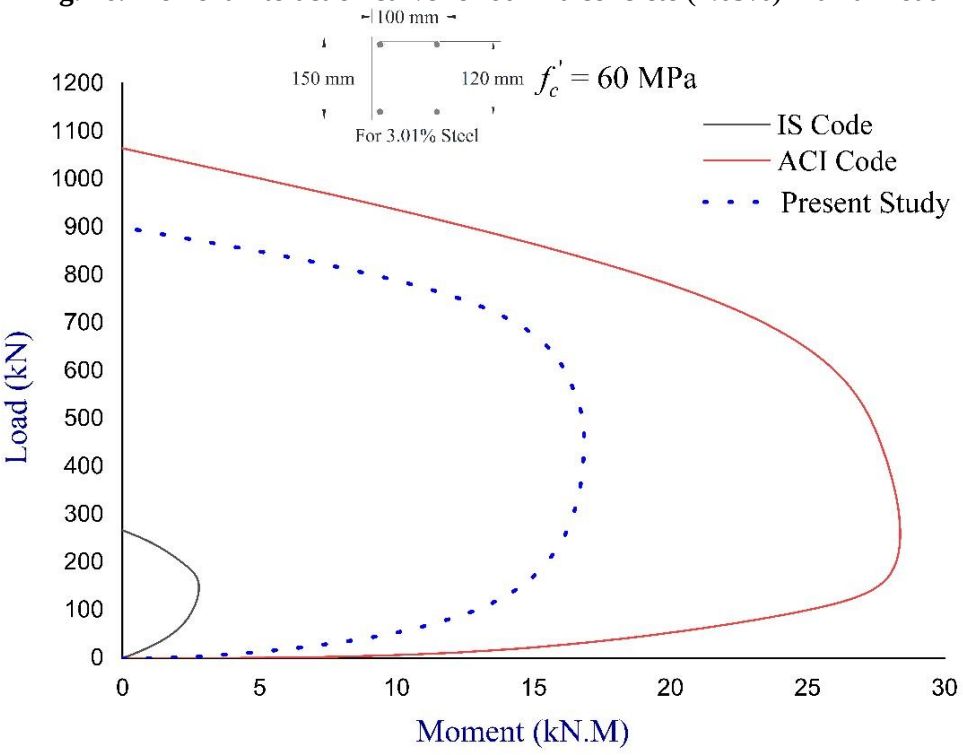

Fig. 17. Moment Interaction curve for 60MPa concrete (3.01%) Biaxial Loading

Similarly, the moment Interaction curves are drafted for M70 and M80 grade concrete column subjected to uniaxial and biaxial loading for 1.34%, 2.09% and 3.01%. These curves showcase the relationship between the axial load (compression or tension) and the bending moment (resulting from external loads) that a column can sustain before failure. Each curve represents a specific combination of axial load and bending moment that the column can withstand without failing. These curves provide engineers with essential information to design columns within safe limits considering both axial and bending loads. understanding these moment interaction curves is crucial for structural engineers and designers. It helps them in designing columns that

can safely support the expected loads while considering different concrete grades, loading conditions, and reinforcement ratios. It aids in making informed decisions about the size, reinforcement, and overall structural integrity of the columns in various construction projects.

6. Conclusions

Different series of specimens such as plain column with fixed neutral axis as tested by Hognestad et al. (1955), eccentrically loaded columns and beams in pure flexure are tested and stress block parameters are arrived. In addition to the stress-block parameters with respect to cylindrical strength the authors have proposed them with respect to cube strength. Some mechanical properties are also studied and the following conclusions are drawn for the strength of concrete in the range of 60MPa to 80MPa.

1. The literature and present study indicate the ratio of cylinder compressive strength and cube compressive strength, increases as strength increases. In the proposed study it is assumed to be 0.80 for NSC and 0.85 for HPC.
2. Equations as proposed in IS 456 underestimates the modulus of rupture and on the other hand overestimates modulus of elasticity for HPC. Hence, they may be modified to represent HPC.
3. The authors feel that the equivalent rectangular stress block is better represents HPC than the parabolic. This also avoids tedious calculations in predicting column capacities in flexure.
4. The stress-block parameters for HPC with respect to cube compressive strength are proposed and are,

$$\alpha_1 = 0.75 - \frac{1}{1000}\left(f_{cu} - 20\right) \quad 0.75 \geq \alpha \geq 0.69$$

$$\beta_1 = 0.85 - \frac{1}{600}\left(f_{cu} - 20\right) \quad 0.85 \geq \beta \geq 0.67$$

5. In future revisions of IS 456 (2000) the results of the present study may be considered.

References

1. Sarjin M, Ghosh S K, Handa V K 1971 Effects of lateral reinforcement upon the strength and deformation properties of concrete. Mag. Concrete Rec., 23: pp 99-110
2. Karsan I D, Jisra J O 1970 Behavior of concrete under varying strain gradient. Journal of Structural Engineering, ASCE, 97: 1969-1990
3. Saatcioglu M, Salamat A H, Razvi S R 1995 Confined columns under eccentric loading. Journal of Structural Engineering, ASCE, 121: 1547-1556
4. Mast R F, Dawood M, Rizkalla S H, Zia P 2008 Flexural strength design of concrete beams reinforced with high-strength steel bars. ACI Structural Journal, 105: 570-577
5. Shahrooz M Bahram et. al. 2009 Flexural behavior and design with high-strength bars and those without well-defined yield point. TRB 2010 Annual Meeting CD-ROM
6. Tan T H, Nguyen N 2005 Flexural behavior of confined high-strength concrete columns. ACI Structural Journal, 102: 198-205
7. Pornchai Jiratatprasot 2002 Mechanical properties and stress-strain behavior of high-performance concrete under uniaxial compression, A Thesis submitted for the degree of Master of Science in Civil Engineering, New Jersey Institute of Technology
8. Wee T H, Chin M S, Manasur M A 1996 Stress-strain relationship of high-strength concrete in compression. Journal of Materials In Civil Engg, 70-76
9. . Kaar P H, Hanson N W, Capell H T 1977 Stress-strain characteristics of high-strength concrete. Research and Development Bulletin RD051 01D, Portaland Cement Association, Skokie, III.
10. 1Sungjoong Kim, 2007 Behavior of high strength concrete columns, Ph. D. dissertation, Raleigh, North Carolina, 205
11. Nedderman H 1973 Flexural stress distribution in very high-strength concrete, MAsc thesis, Dept. of Civil Engineering, Univ. of Texas, Arlington, Tex
12. NZS 3101 2006 The Design of Concrete Structures, Standards New Zealand, Wellington, New Zealand, 520
13. AS 3600 2001 Concrete Structures, Standards Australia, Home burls, NSW, Australia
14. Neville A M 1981 Properties of concrete, The English Language Book Society and Pitman, Third Edition
15. Aitcin P C 1998. High-performance Concrete. E & FN Spon. An imprint of Routledge 11 New Fetter Lane, London,
16. Aitcin, P. C. (1998). High performance concrete. CRC press.
17. Aitcin, P. C. (2018). The use of superplasticizers in high performance concrete. In High Performance Concrete (pp. 14-33). CRC Press.
18. AKELILU, M. E. (2021). Experimental investigation on properties of mortar

containing waste marble and fly ash (Doctoral dissertation).
19. American Concrete Institute (ACI). ACI 318-08 Building Code and Commentary, Farmington Hills MI, 2008, 430
20. Amran, M., Huang, S. S., Onaizi, A. M., Makul, N., Abdelgader, H. S., & Ozbakkaloglu, T. (2022). Recent trends in ultra high-performance concrete (UHPC): Current status, challenges, and future prospects. Construction and Building Materials, 352, 129029. https://doi.org/10.1016/j.conbuildmat.2022.129029
21. Amran, M., Onaizi, A. M., Fediuk, R., Danish, A., Vatin, N. I., Murali, G., & Azevedo, A. (2022). An ultra-lightweight cellular concrete for geotechnical applications–A review. Case Studies in Construction Materials, 16, e01096. https://doi.org/10.1016/j.cscm.2022.e01096
22. Attard M M, Stewart M G 1998 A two parameter stress-block for high-strength concrete. ACI Struct. J., 95: 305-317
23. Awati, M., & Khadiranaikar, R. B. (2012). Behavior of concentrically loaded high performance concrete tied columns. Engineering structures, 37, 76-87. https://doi.org/10.1016/j.engstruct.2011.12.040
24. Bae Sungjin, Bayrak Oguzhan 2003a Early cover spalling in high-strength concrete columns. J. Struct. Eng., 29: 314-323
25. Bae Sungjin, Bayrak Oguzhan 2003b Stress block parameters for high strength concrete members. ACI Struct. J., 100: 626-636
26. Canbay Erdem, Ozcebe Guney, Ersoy Ugur 2006 High-strength concrete columns under eccentric load. J. Struct. Eng., 132: 1052-1060
27. Chekravarty, D. S. V. S. M. R. K., Mallika, A., Sravana, P., & Rao, S. (2022). Effect of using nano silica on mechanical properties of normal strength concrete. Materials Today: Proceedings, 51, 2573-2578. https://doi.org/10.1016/j.matpr.2021.12.409
28. Cheng, X., Du, H., Shi, X., & Mansour, M. (2023). Ultimate biaxial bending resistance of H-section steel members under different loading paths. Journal of Constructional Steel Research, 200, 107678. https://doi.org/10.1016/j.jcsr.2022.107678
29. Cormack H W 1956 Notes on cubes versus cylinders. New Zealand Engineering (Wellington), 11: 98-99
30. Dharmaraj, R., Bhadauria, S. S., Mayilsamy, K., Thivya, J., Karthick, A., Baranilingesan, I., ... & Osman, S. M. (2022). Investigation of Reinforced Concrete Column Containing Metakaolin and Fly Ash Cementitious Materials. Advances in Civil Engineering, 2022, 1-13. https://doi.org/10.1155/2022/1147950
31. Dinakar, P., Sethy, K. P., & Sahoo, U. C. (2013). Design of self-compacting concrete with ground granulated blast furnace slag. Materials & Design, 43, 161-169. http://dx.doi.org/10.1016/j.matdes.2012.06.049
32. Elsayed, M., Tayeh, B. A., Abou Elmaaty, M., & Aldahshoory, Y. (2022). Behaviour of RC columns strengthened with Ultra-High Performance Fiber Reinforced concrete (UHPC) under eccentric loading. Journal of Building Engineering, 47, 103857. https://doi.org/10.1016/j.jobe.2021.103857
33. Elwell D J, Fu Gongkang 1995 Compression testing of concrete: Cylinders vs. Cubes. Special report 119, Transportation research and development Bureau, Albany, New York
34. Elwi, A. E., Begum, M., & Driver, R. G. (2007). Numerical simulations of the behaviour of partially encased composite columns.
35. Envas R H 1944 The plastic theories for the ultimate strength of reinforced concrete beams. Journal of the Institution of Civil Engineers (London), 21: 98-121
36. Foster S J, Attard M M 1997 Experimental tests on eccentrically loaded high strength concrete columns. ACI Struct. J., 94: 295-303
37. Gonnerman H F 1925 Effect of size and shape of test specimen on compressive strength of concrete. Proc. ASTM, 25: 237-250
38. Hognestad E 1951 A study of combined bending and axial load in reinforced concrete members. Engineering experiment station., Bulletin No. 399, Univ. of Illinois, Urbana, III.
39. Hognestad E 1952 Inelastic behavior in tests of eccentrically loaded short reinforced columns. J. Am. Concr. Inst., 24: 117-139
40. Hognestad E, Hanson N W, McHenry D 1955 Concrete stress distribution in ultimate strength design. J. Am. Concr. Inst., 52: 455-479
41. Ibrahim H H H, MacGregor J G 1996 Tests of eccentrically loaded high-strength concrete columns. ACI. Struct. J., 93: 585-594
42. Ibrahim H H H, MacGregor J G 1997 Modification of the ACI rectangular stress block for high-strength concrete. ACI Struct. J., 94: 40-48

43. Indian standards (IS-12269) 1987 Specifications for 53-grade ordinary Portland cement. Bureau of Indian Standards, New Delhi
44. Indian standards (IS-383) 1970. Testing aggregates in cement concrete. Bureau of Indian Standards, New Delhi
45. Indian standards (IS-456) 2000 Indian standard code of practice for plain and reinforced concrete (Fourth Revision). Bureau of Indian Standards, New Delhi
46. Iravani Said 1996 Mechanical properties of high-performance concrete. ACI Materials Journal, 93-M47: 416-426
47. Lee Jae-Hoon, Son Hyeok-soo 2000 Failure and strength of high-strength concrete columns subjected to eccentric loads. ACI. Struct. J., 97: 75-85
48. Lloyd N A, Rnagan B V 1996 Studies on high-strength concrete columns under eccentric compression. ACI. Struct. J., 93: 631-638
49. Metrol H C, Rizkalla S, Zia P, Mirmiran A 2008 Characteristics of compressive stress distribution in high-strength concrete. ACI. Struct. J., 105: 626-633
50. Murty C V R 2001 Shortcomings in structural design provisions of IS 456-2000. Indian Concrete Journal, Point of View, 150-157
51. Muttock A H, Kriz L B, Hognestad E 1961 Rectangular concrete stress distribution in ultimate strength design. J. Am. Concr. Inst., 57: 875-928
52. Rűsch H 1955 Tests on the strength of the flexural compression zone, Bulletin No 9.120. Deutsher Ausschuss Fur Stahlbeton. Berlin
53. Swartz S E, Nikaeen A, Narayan Babu H D, Periyakaruppan N, Refai T M E 1985 Structural bending properties of high strength concrete. ACI SP., 87: 147-178
54. Nayak, C. B., Wadgave, P. (2016). vibrational analysis of chimney Equipped with strakes and tune mass Damper. Journal of International Journal for Sci. Research and Development, 4, 321-333.
55. Nayak, C. B., Nerkar, S. (2016). Seismic behaviour of elevated storage reservoir by finite element method. Journal of International Journal for Sci. Research and Development, 4(1), 1188-1197.
56. Nayak, C. B., Kharjule, K. (2016). Lateral analysis of elevated reinforced concrete silos. Journal of International journal of pure and Applied research in engineering and Technology, 4(9), 411-421.
57. Togay Ozbakkaloglu, Saatcioglu Murat 2004 Rectangular stress block for high-strength concrete. ACI Struct. J., 101: 475-483
58. Venkatasubramani, Yohanna Jibi, Prameswaran 2007 Analytical and experimental investigations on eccentrically loaded slender reinforced concrete columns. Journal of structural engineering, 33: 391-400
59. Whitney C S 1937 Design of reinforced concrete members under flexure and combined flexure and direct compression. J. Am. Concr. Inst., 33: 483-498
60. Wu Ke-Ru, Chen Bing, Yao Wu, Dong Zhang 2001 Effect of coarse aggregate type on mechanical properties of High-performance Concrete. Cement and Concrete Research, 31: 1421-1425
61. Zhenhua Wu 2006 Behavior of high-strength concrete members under pure flexure and axial-flexural loadings, PhD dissertation, Univ. North Carolina, Raleigh.